9-1-2018

Characterization of the mature form of a β-defensin-like peptide, Hoa-D1, in the lobster Homarus americanus

Giap H. Vu
Bowdoin College

Daniel Do
Bowdoin College

Cindy D. Rivera
Bowdoin College

Patsy S. Dickinson
Bowdoin College

Andrew E. Christie
Pacific Biosciences Research Center

See next page for additional authors

Molecular Immunology 101 (2018) 329–343

Contents lists available at ScienceDirect

Molecular Immunology

journal homepage: www.elsevier.com/locate/molimm

Characterization of the mature form of a β-defensin-like peptide, *Hoa*-D1, in the lobster *Homarus americanus*

Giap H. Vu[a], Daniel Do[a], Cindy D. Rivera[a], Patsy S. Dickinson[b], Andrew E. Christie[c], Elizabeth A. Stemmler[a,*]

[a] Department of Chemistry, Bowdoin College, 6600 College Station, Brunswick, ME 04011, United States
[b] Department of Biology, Bowdoin College, 6500 College Station, Brunswick, ME 04011, United States
[c] Békésy Laboratory of Neurobiology, Pacific Biosciences Research Center, School of Ocean and Earth Science and Technology, University of Hawaii at Manoa, 1993 East-West Road, Honolulu, HI 96822, United States

ARTICLE INFO

Keywords:
Antimicrobial peptide
Defensin
Homarus americanus
Hemolymph
Chip-based nanoLC-QTOF-MS/MS
Transcriptomics

ABSTRACT

We report on the characterization of the native form of an American lobster, *Homarus americanus*, β-defensin-like putative antimicrobial peptide, *H. americanus* defensin 1 (*Hoa*-D1), sequenced employing top-down and bottom-up peptidomic strategies using a sensitive, chip-based nanoLC-QTOF-MS/MS instrument. The sequence of *Hoa*-D1 was determined by mass spectrometry; it was found to contain three disulfide bonds and an amidated C-terminus. The sequence was further validated by searching publicly-accessible *H. americanus* expressed sequence tag (EST) and transcriptome shotgun assembly (TSA) datasets. *Hoa*-D1, SYVRScSSNGGDcVYRcYGNIINGAcSGSRVccRSGGGYamide (with c representing a cysteine participating in a disulfide bond), was shown to be related to β-defensin-like peptides previously reported from *Panulirus japonicas* and *Panulirus argus*. We found *Hoa*-D1 in *H. americanus* hemolymph, hemocytes, the supraoesophageal ganglion (brain), eyestalk ganglia, and pericardial organ extracts, as well as in the plasma of some hemolymph samples. Using discontinuous density gradient separations, we fractionatated hemocytes and localized *Hoa*-D1 to hemocyte sub-populations. While *Hoa*-D1 was detected in semigranulocytes and granulocytes using conventional proteomic strategies for analysis, the direct analysis of cell lysates exposed evidence of *Hoa*-D1 processing, including truncation of the C-terminal tyrosine residue, in the granulocytes, but not semigranulocytes. These measurements demonstrate the insights regarding post-translational modifications and peptide processing that can be revealed through the MS analysis of intact peptides. The identification of *Hoa*-D1 as a widely-distributed peptide in the lobster suggests the possibility that it may be pleiotropic, with functions in addition to its proposed role as an antimicrobial molecule in the innate immune system.

1. Introduction

The American lobster, *Homarus americanus*, is a commercially important species, playing a key economic role in fishing communities in both New England and Atlantic Canada. This species is also widely used as a model organism (Marder and Bucher, 2007), providing insights into the mechanisms that produce and modulate rhythmic motor patterns. As environmental and anthropogenic stresses to marine populations increase, greater attention is being directed at the study of infectious diseases in marine organisms (Maynard et al., 2016), with aims to better understand, forecast, and manage disease outbreaks (Cawthorn, 2011). Although limited information is available regarding the humoral immune response in *H. americanus*, a number of recent bioinformatics studies have begun to identify changes in gene expression in response to bacterial, parasitic, and viral challenges (Beale et al., 2008; Clark et al., 2013a,b,c).

Antimicrobial peptides (AMPs) function as essential components of the innate immune response in invertebrate species (Balandin and Ovchinnikova, 2016; Smith and Dyrynda, 2015). AMPs, which generally have broad-spectrum antimicrobial effects, are smaller molecules (often less than 10-kDa) that exhibit both hydrophobic and cationic character and exert their activity, in many instances, by interacting with the membranes of pathogens (Schmitt et al., 2016; Shai, 2002). Crustacean AMPs offer possibilities towards addressing current

Abbreviations: nanoESI, nanoelectrospray ionization; nanoLC, nano-liquid chromatography; QTOF-MS/MS, quadrupole time-of-flight-mass spectrometry/mass spectrometry; AMP, antimicrobial peptide; CID, collision induced dissociation; TIC, total ionization chromatogram; EIC, extracted ion chromatogram; MWCO, molecular weight cut off; DTT, dithiothreitol; IAA, iodoacetamide; EST, expressed sequence tag; TSA, transcriptome shotgun assembly

* Corresponding author.
E-mail address: estemmle@bowdoin.edu (E.A. Stemmler).

https://doi.org/10.1016/j.molimm.2018.07.004
Received 9 February 2018; Received in revised form 30 June 2018; Accepted 2 July 2018
Available online 20 July 2018

limitations in the treatment of infections in humans and animals, and have served as structural models for the design and development of potential therapeutics (Hancock et al., 2006). AMPs derived from marine sources have garnered special attention because marine organisms exist in environments rich in potentially pathogenic microbes, raising expectations that, in response, highly effective AMPs have evolved (Sperstad et al., 2011). This has motivated work resulting in the isolation of novel AMPs from a variety of marine sources (Kang et al., 2015). While both *H. amerianus* hemocytes (Battison et al., 2008) and cuticle (Mars Brisbin et al., 2015) have been found to exhibit antimicrobial activity, the molecular identities of the active components in these tissues have not been conclusively established.

The majority of AMPs identified in crustaceans have been characterized via the identification of genes and gene expression signatures (e.g. Afsal et al., 2013; Antony et al., 2011; Christie et al., 2007; Donpudsa et al., 2010; Liu et al., 2016; Sperstad et al., 2011), frequently exploiting sensitive and high dynamic range nucleotide sequencing and bioinformatics approaches. Mass spectrometry (MS)-based proteomic or peptidomic strategies reveal information not provided by genetics (Kumar et al., 2016), including unique information about post-translational modifications that can be key to biological activity and regulation of biological pathways; however, very few studies directed at the identification of crustacean AMPs have employed MS-based strategies.

Recently, the genes for two isoforms of a defensin-like peptide from the spiny lobster *Panulirus argus* were sequenced; they were shown, using phylogenetic analysis, to be related to ancestral β-defensins from vertebrates (Montero-Alejo et al., 2012). A defensin-like peptide, named panusin, was subsequently isolated from hemocytes of *P. argus* and was found to have broad-spectrum antimicrobial activity (Montero-Alejo et al., 2017). In this study, we report the structural characterization of the native form of a β-defensin-like peptide from *H. amerianus*, which was named *H. americanus* defensin 1 (*Hoa*-D1). We have employed a high sensitivity, microfluidics chip-based nanoLC-QTOF-MS/MS (Yin and Killeen, 2007; Yin et al., 2005) approach to the analyses, making use of an on-chip enrichment/desalting column for analyte preconcentration, followed by low flow (300 nL/min) analytical separation to permit nanoelectrospray ionization (nanoESI) of separated extract components. Using this approach, we have detected *Hoa*-D1 as an abundant, lower molecular mass component of *H. americanus* hemocytes, heat-treated hemolymph, *H. americanus* nervous system tissue extracts and some hemocyte-free plasma samples. Both top-down and bottom-up peptidomic strategies were employed to sequence *Hoa*-D1 and to localize the peptide to different tissues and hemocyte subpopulations. Cumulatively, this study presents evidence for a widely distributed AMP from *H. americanus*. Furthermore, this work demonstrates how a chip-based nanoLC-MS technique, applied for the first time to the direct analysis of intact peptides in hemolymph samples from a marine crustacean, can provide information regarding post-translational modifications and other forms of peptide processing, information that can not be discerned from genetic information or the application of conventional proteomic strategies.

2. Materials and methods

2.1. Animals and hemolymph collection

American lobsters, *H. americanus*, were purchased from local suppliers (Brunswick and Harpswell, ME, USA); they were maintained in aerated seawater tanks at 8–10 °C, and were fed weekly with chopped squid or shrimp. Prior to hemolymph or tissue collection, animals were anaesthetized by packing in ice for approximately 30 min. Hemolymph (0.5–5.0 mL) was withdrawn directly from the pericardial cavity or from the ventral hemolymph sinus, which was accessed through the ventral base of the coxa of the third walking leg, and placed into 1.5 or 15 mL centrifuge tubes.

2.2. Heat-treated and coagulated hemolymph samples

To heat-treat samples, hemolymph (0.5 mL) was immediately heated at 100 °C for 5 min. The samples were then homogenized and centrifuged at 14.5 krpm (Eppendorf MiniSpin Plus) for 15 min at room temperature and the supernatant (~400 μL) was collected and stored at −20 °C until analysis. Serum (liquid component) isolated from coagulated hemolymph was collected following the centrifugation of coagulated hemolymph (0.5 mL) at 14.5 krpm for 15 min at 4 °C. The serum (~150 μL) was stored at −20 °C until analysis.

2.3. Hemocyte collection and fractionation

To separate hemocytes from the liquid component of uncoagulated hemolymph (plasma), hemolymph was mixed in a 1:1 vol ratio with chilled anticoagulant (0.45 M NaCl, 0.1 M glucose, 30 mM trisodium citrate, 6 mM citric acid, 10 mM EDTA in water (Fisher; LCMS grade), pH 4.6). Mixed hemocytes were isolated from hemolymph (0.5 mL) after mixing with anticoagulant and centrifuging at 750 × *g* (Micro Centrifuge 5415 C, Eppendorf) for 15 min at 4 °C. The plasma was removed and the cell pellet was washed twice with 200 μL of fresh, chilled anticoagulant and centrifuged at 750 × *g* for 5 min at 4 °C. Isolated hemocytes were lysed or stored at −80 °C.

For some experiments, hemocytes were separated into three fractions assigned as granulocytes (G), semigranulocytes (SG) and hyalinocytes (H) cells using discontinuous density gradient centrifugation with 80%, 60%, and 30% (v/v) Percoll (GE Healthcare Bio-Sciences, Pittsburgh, PA), diluted with 0.45 M NaCl. Percoll layers (2 mL each) were prepared in a 15 mL centrifuge tube. Hemolymph (4 mL) was mixed 1:1 with chilled anticoagulant, stacked on top of the gradient and centrifuged in a swinging-bucket centrifuge (Allegra X-30R, Beckman Coulter Life Sciences) at 2.7 krpm for 40 min at 7 °C with the acceleration and brake turned off. Bands of fractionated hemocytes were carefully aspirated and transferred into new 15 mL tubes. The Percoll solution was removed by mixing the cells with five volumes of chilled anticoagulant, followed by 15 min of centrifugation at 2.8 krpm to pelletize the hemocytes. This washing procedure was repeated a second time and the pelletized, fractionated hemocytes were lysed or stored at −80 °C.

2.4. Hemocyte microscopy

Hemocytes (mixed or fractionated) were suspended in anticoagulant (5–10 μL) and visualized immediately after collection with a BX51 digital microscope (Olympus) using bright-field illumination. An Evolution VF Color digital camera (Media Cybernetics, Silver Spring, MD) with the accompanying QCapture Suite 99PLUS software (QImaging Corporation, Burnaby, BC, Canada) was used to capture images with a total magnification of 400×. Images were prepared for publication using Fiji (Schindelin et al., 2012), an open source image processing program.

2.5. Hemocyte extraction and protein quantification

Mixed or fractionated hemocytes were lysed with a motorized-pestle mixer (Argos Technologies) using 200 μL of lysis buffer (8 M urea (SigmaAldrich) and 1 M ammonium bicarbonate (SigmaAldrich)) and centrifuged at 16.5k × *g* (Micro Centrifuge 5415 C, Eppendorf) for 60 min at 4 °C. The supernatant was stored at −20 °C until analysis. Protein concentrations were determined via microplate DC Lowry Assay per manufacturer's procedure (Bio-Rad, Hercules, CA) using a SPECTROstar Nano Absorbance plate reader (BMG LABTECH Inc, Cary, NC). Bovine serum albumin (BSA) prepared in lysis buffer was used as the protein calibration standard.

In preparation for the LC/MS analysis of intact peptides, 30 kDa MWCO filters (Amicon Ultra-0.5 mL; Millipore) were used to remove

higher molecular mass components from the samples. The flow-through from the filters was desalted and concentrated using Pierce™ C18 Spin Columns (Thermo Fisher Scientific).

2.6. Tissue collection and sample preparation

Supraoesophageal ganglion (brain), eyestalk ganglia, and pericardial organs (PO) from individual lobsters were isolated via manual microdissection in chilled (8–10 °C) physiological saline (composition in mM: NaCl, 479.12; KCl, 12.74; $CaCl_2$, 13.67; $MgSO_4$, 20.00; Na_2SO_4, 3.91; Trizma base, 11.45; maleic acid, 4.82 [pH, 7.45]). To deactivate proteolytic enzymes (Stemmler et al., 2013), tissues were placed in 58 µL of LCMS water (Fisherbrand) in a 1.5 mL low retention tube that was heated at 100 °C for 5 min. Heat-treated tissues were homogenized and extracted following the addition of methanol (LCMS-grade; Fisherbrand; 128 µL) and glacial acetic acid (reagent grade; SigmaAldrich, ≥ 99%; 14 µL). The tissues were homogenized using a motor-driven tissue grinder equipped with a polypropylene pestle (SigmaAldrich). Following homogenization, the tissues were sonicated for 5 min and centrifuged at 14.5 krpm for 5 min. The supernatant was removed from the tissue and the remaining tissue was re-suspended in 50 µL of extraction solvent (30% water; 65% methanol; 5% glacial acetic acid), sonicated for 5 min, centrifuged at 14.5 krpm for 5 min; the supernatant was again removed. The supernatants were combined and filtered through 10- or 30-kDa MWCO filters (Amicon Ultra-0.5 mL; Millipore) that had been prewashed with two 200-µL volumes of extraction solvent. The MWCO filters were centrifuged at 14.5 krpm for 20 min. The flow-through (approximately 350 µL) was collected for further processing or analysis. Brain, eyestalk ganglia, or PO extracts (350 µL) were dried using a SpeedVac vacuum concentrator (UVS400 Universal Vacuum System, Thermo Electron Corporation) at 36 °C prior to analysis.

2.7. Peptide isolation using reversed-phase HPLC

Hoa-D1 was isolated from the supernatant of the heat-treated hemolymph using an Agilent Technologies 1260 Infinity HPLC system equipped with a diode-array detector (DAD) (G4212B) and a fraction collector (G1364C). A 250 × 2.0 mm Jupiter, Proteo, 90-Å, microbore C_{18} column (Phenomenex, Torrance, CA), packed with 4 µm particles, was used for the separation. A 4.0 × 2.0 mm MAX-RP guard column (Phenomenex) was attached to the input end of the separation column. Mobile phase A was 0.1% trifluoroacetic acid in water (HPLC-grade; Fisher Scientific); mobile phase B was 0.1% trifluoroacetic acid in acetonitrile (HPLC-grade; Fisher Scientific). A gradient of 98% A (0 min), 80% A (15 min), 80% A (25 min), 0% A (25.1 min), 0% A (30 min) with a flow rate of 0.2 mL/min was used to fractionate 100 µL injections of heat-treated hemolymph. *Hoa*-D1 was collected in one fraction that eluted from 22.9 to 23.3 min. This fraction was dried in a Speedvac (UVS400 Universal Vacuum System, Thermo-Electron Corporation) at 36 °C and reconstituted with LCMS-grade water.

2.8. Reduction of disulfide bonds and alkylation of free sulfhydryl groups

Dithiothreitol (DTT; SigmaAldrich) in ammonium bicarbonate (AmBic; SigmaAldrich; > 99.5% purity) buffer was added to each sample of interest, such that the final concentrations of DTT and AmBic in the sample were 35 mM and 25 mM, respectively and the pH was between 8-8.5. The samples were then incubated at room temperature in the dark for 1 h (fractionated peptide) or at 90 °C for 1 h (tissue or hemocyte extracts), in order to completely reduce all disulfide bonds.

Iodoacetamide (IAA; SigmaAldrich) in AmBic buffer was added to the reduced sample, such that the final concentrations of IAA and AmBic in the sample were 10.5 mM and 25 mM, respectively. The sample was incubated at room temperature, in the dark, for 1 h, in order to completely alkylate all free sulfhydryl groups. An additional equivalent of DTT was added to the alkylated sample to quench residual IAA, in order to prevent over-alkylation.

2.9. Enzymatic digestion

A 5 µL aliquot containing 1.25 ng of bovine trypsin (SigmaAldrich), buffered with 25 mM AmBic, was added to 72 µL of the reduced alkylated peptide sample. For the heat-treated hemolymph, 12.5 ng of bovine trypsin was added to every 30 µL (1/20th) of sample. The sample was then incubated at 37 °C for 12 h, and stored at −20 °C until analysis.

2.10. Gel electrophoresis

Mixed and fractionated hemocyte lysates were prepared for sodium dodecyl sulfate-polyacrylamide gel electrophoresis (SDS-PAGE) by mixing 35 µg of protein in hemocyte lysate in a 1:1 vol ratio with 2X Laemmli Sample Buffer (Bio-Rad) containing 100 mM DTT. Samples were heated at 100 °C for 5 min and loaded onto 4–20% Mini-PROTEAN TGX Precast Protein Gradient Gels (Bio-Rad) using Precision Plus Protein Dual Xtra Prestained Protein Standards (Bio-Rad) as the molecular weight markers. Proteins were separated by applying 95 V for the first 30 min, 145 V for the next 45 min, with a final application of 200 V, which was terminated when the dye front reached the end of the gel. The gel was rinsed in deionized water and fixed in a solution of 40% methanol and 10% glacial acetic acid in deionized water for 45–60 min with gentle shaking. After fixing, the gel was rinsed with deionized water and stained in a solution of 45% methanol, 10% acetic acid, and 0.25% (w/v) Coomassie Brilliant Blue R-250 (Bio-Rad) in deionized water for 60–90 min with gentle shaking. The stained gel was then washed in the fixing solution for approximately 2 h with gentle shaking. The gel was backlit on a light box and documented with an iPhone camera.

2.11. In-gel digestion

The targeted gel bands were excised from the gel, sliced into small pieces and placed into 0.6 mL microcentrifuge tubes. The gel was destained using three washes of 400 µL destain solution (50% acetonitrile in 25 mM AmBic), applied for 10 min, followed by a wash with 400 µL of 100% acetonitrile for 10 min. After removing the acetonitrile, the gel pieces were dehydrated in a Speedvac for 20 min. DTT (100 µL; 10 mM) was added and heated at 55 °C for 45 min. After the solution was removed, IAA (100 µL; 55 mM) was reacted at room temperature for 45 min. After the solution was removed, the gel was washed with 400 µL of 50% acetonitrile in 25 mM AmBic, followed by a second wash with 100 µL of 50% acetonitrile in 25 mM AmBic. After washing with 400 µL of 100% acetonitrile, the gel pieces were dried in a Speedvac for 20 min. Sequencing grade modified trypsin (Promega; 20 µL of 10 ng/µL stock in 25 mM AmBic) was added to each vial. The tubes were left on ice for 10 min. Additional 25 mM AmBic was added to cover the gel pieces and the tubes were incubated at 37 °C for 14 h. Peptides were extracted by first transferring the solution to a clean microcentrifuge tube. Extraction solution (30 µL; 50% acetonitrile, 5% formic acid) was added and the tubes were sonicated 5 min and centrifuged. The solution was removed and this process was repeated. The collected solutions were dried with a Speedvac and reconstituted in 40 µL of 0.1% formic acid in water for LC/MS/MS analysis. Protein identification was conducted as described in *Data analysis*, below.

2.12. Chip-based nanoLC-QTOF-MS/MS

Mass spectrometric analysis was performed using a 6530 quadrupole time-of-flight (Q-TOF) mass analyzer (Agilent Technologies, Santa Clara CA). Mass spectra (MS and MS/MS) were collected in positive ion mode; the ionization voltage ranged from 1850 to 1975 V and the ion source temperature was held at 350 °C. Spectra were internally

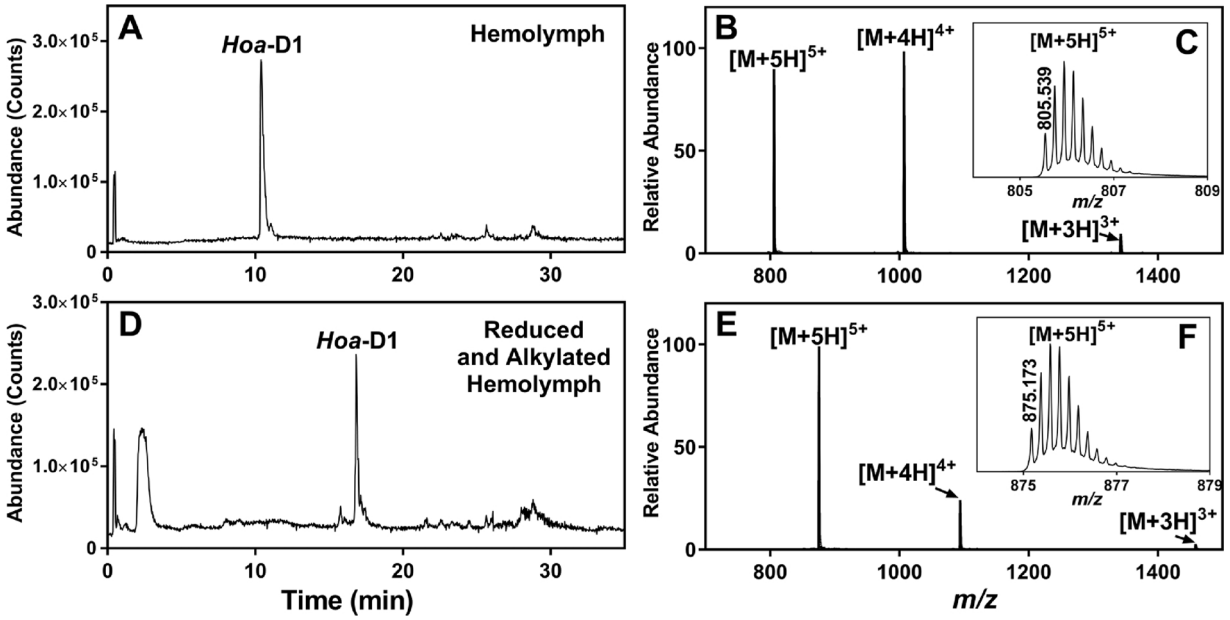

Fig. 1. (A) Total ionization chromatogram (TIC) for supernatant isolated from heat-treated hemolymph after centrifugation; (B) nanoESI mass spectrum of *Hoa*-D1; (C) expansion showing the isotopic pattern for the $[M+5H]^{5+}$ ion for *Hoa*-D1; (D) TIC for supernatant isolated from heat-treated hemolymph following reduction and alkylation with iodoacetamide; (E) nanoESI mass spectrum of reduced and alkylated *Hoa*-D1; (F) expansion showing the isotopic pattern for the $[M+5H]^{5+}$ charge state for *Hoa*-D1. The shift in retention time for the reduced and alkylated peptide results from the increased hydrophobicity associated with conversion of disulfide bonds to alkylated cysteine residues; the shift from a monoisotopic mass of 4022.66 Da (native) to 4370.84 Da (reduced and alkylated) reveals that *Hoa*-D1 has three disulfide bonds and six cysteine residues.

calibrated using dibutyl phthalate ($C_{16}H_{22}O_4$) and hexakis(1H,1H,4H-hexafluorobutyloxy)phosphazine (HP-1221; $C_{24}H_{18}O_6N_3P_3F_{36}$), continuously evaporated and detected as $[M+H]^+$. CID-MS/MS experiments were executed with precursor ions subjected to collision-induced dissociation (CID) using nitrogen as the target gas.

Chromatographic separation and nanoelectrospray ionization (nanoESI) were performed using a 1260 Chip Cube system (Agilent Technologies) and a ProtID-chip with a 40 nL enrichment column and a 43- or 150-mm × 75 µm analytical column (Agilent Technologies). The enrichment and analytical columns were packed with 300 Å, 5 µm particles with Zorbax 300SB-C18 stationary phase. The mobile phases were 0.1% formic acid in H_2O (A) and 0.1% formic acid and 2% water in acetonitrile (B). Samples (1–8 µL) were loaded on the enrichment column using 98:2 (A:B) at 4 µL/min. The tryptic digests of HPLC-fractionated *Hoa*-D1 were analyzed with the 43-mm analytical column using a gradient of 98:2 (A:B) for 1 min to 65:35 (A:B) at 60 min at 0.3 µL/min. The remaining samples were analyzed with the 150-mm analytical column using a linear gradient of 98:2 (A:B) for 1 min to 65:35 (A:B) at 40 min, to 30:70 (A:B) at 45 min and 2:98 (A:B) at 45.1 min using a flow rate of 0.3 µL/min.

2.13. Transcriptome mining

2.13.1. Database searches

Database searches were conducted on or before October 23, 2016, using methods modified from a well-vetted protocol (e.g. Christie, 2016a,b; Christie and Pascual, 2016). Specifically, the database of the online program tblastn (National Center for Biotechnology Information, Bethesda, MD; http://blast.ncbi.nlm.nih.gov/Blast.cgi) was set to either "Expressed Sequence Tags (EST)" or "Transcriptome Shotgun Assembly (TSA)" and restricted to data from *H. americanus* "(taxid:6706)". The sequence of the putative *H. americanus* defensin identified via mass spectrometry (see Results), with a carboxyl (C)-terminal glycine added because of its predicted amidation, was used as the BLAST query sequence.

2.13.2. Peptide prediction

All BLAST hits returned for a given database search were fully translated using the "Translate" tool of ExPASy (http://web.expasy.org/translate/), and then checked manually for homology to the query sequence. The structures of putative mature defensin peptides were predicted using a workflow developed for the identification of neuropeptides (e.g. Christie, 2016a, b; Christie and Pascual, 2016). Specifically, each of the deduced precursor proteins was assessed for the presence of a signal peptide using the online program SignalP 4.1 (http://www.cbs.dtu.dk/services/SignalP/; (Petersen et al., 2011); the D-cutoff values of SignalP 4.1 were set to "Sensitive" to better match the sensitivity of version 3.0 of this freeware program. Prohormone cleavage sites were identified based on the information presented in Veenstra (Veenstra, 2000) and/or by homology to known arthropod pre/preprohormone processing schemes. The sulfation states of tyrosine residues were predicted using the online program "Sulfinator" (http://www.expasy.org/tools/sulfinator/; (Monigatti et al., 2002), while disulfide bonding between cysteine residues was predicted using the online program "DiANNA" (http://clavius.bc.edu/~clotelab/DiANNA/; (Ferre and Clote, 2005); C-terminal amidation at glycine residues was predicted by homology to known arthropod peptide isoforms. All protein/peptide a1ignments were done using the online program MAFFT version 7 (http://mafft.cbrc.jp/alignment/software/; (Katoh and Standley, 2013).

2.14. Data analysis and figure production

Chip-based nanoLC-QTOF-MS/MS figures were generated by exporting Mass Hunter (Agilent) chromatograms or mass spectra as metafiles or text files and importing these data into CorelDRAW X4 or Graphpad Prism 7 for final figure production. Mass spectral deconvolution was executed using the "Deconvolute: Resolved Isotope" tool from the Mass Hunter Qualitative Analysis B.06.00 Software (Agilent). Neutral masses were converted to singly-charged masses for analysis. Protein database searching in conjunction with the analysis of trypsinized samples was performed using Spectrum Mill MS Proteomics

Workbench (Rev. 4.1.141; Agilent Technologies). LC/MS/MS data was searched against an in-house database containing the *Hoa*-D1 sequence and the National Center for Biotechnology Information (NCBI) database.

3. Results and discussion

3.1. Sample preparation

This study reports on the characterization of a peptide (*Hoa*-D1; Fig. 1A) detected in *H. americanus* hemolymph using a chip-based nanoLC-QTOF-MS/MS (Yin et al., 2005) approach. To prepare samples for analysis, a variety of strategies were employed, including (1) analysis of supernatant following heat-treating hemolymph at 100 °C for 5 min, (2) direct analysis of serum following hemolymph coagulation, (3) analysis of hemocytes (mixed or fractionated), which were kept on ice and lysed following isolation in the presence of anticoagulant, and (4) analysis of plasma, following the separation of hemocytes from the plasma. *Hoa*-D1 was consistently detected in samples prepared using heat-treatment and mixed hemocyte extraction (i.e, using strategies (1) and (3)), but was less consistently detected in serum and plasma. Our initial characterization of *Hoa*-D1 made use of heat-treated hemolymph samples.

3.2. Sequencing Hoa-D1 using mass spectrometry

The nanoESI mass spectrum for *Hoa*-D1 showed an abundant $[M+5H]^{5+}$ ion at *m/z* 805.54 (Fig. 1B) with a monoisotopic molecular mass of 4022.65 Da. MS/MS experiments were conducted in an attempt to identify the peptide via top-down *de novo* sequencing using collision induced dissociation (CID); however, only a limited number of useful sequence ions were observed in MS/MS spectra of the +5 and +4 charge states of the peptide using a variety of collision energies (10–70 eV). Using a collision energy of 20 eV, CID of the +5 charge state produced a mass spectrum (Fig. 2A) that showed abundant, but less informative, immonium ions for isoleucine or leucine (I/L; *m/z* 86.10) and tyrosine (Y; *m/z* 136.08). A more informative peak was detected at *m/z* 181.069, a y_1 product ion mass consistent with the combination of C-terminal amidation with tyrosine (Y) as the C-terminal amino acid. This hypothesis was supported by the detection of higher *m/z* ions (*m/z* 1002.414, +4; *m/z* 961.648, +4) resulting from losses of NH_3 and the combination of NH_3 and Y, respectively, as putative b_n and b_{n-1}-type product ions, where n is the total number of amino acid residues in the sequence. Additionally, we detected b_2 and a_2 ions with masses (*m/z* 251.103 and 223.107, respectively) consistent with [SY] as the N-terminus amino acids. While other product ions were detected, including a peak at *m/z* 978.40 (+4) resulting from loss of a isoleucine/leucine (I/L) residue, most peaks resulted from losses of small neutral molecules (CO or H_2O, for example) and did not reveal additional sequence information, even when the peptide was subjected to higher collision energies (up to 70-eV). This suggested to us that efficient peptide fragmentation may have been inhibited by the presence of disulfide bonds.

To determine the number of disulfide bonds and cysteine residues present in *Hoa*-D1, and to promote the production of sequence-informative product ions by CID, we used DTT to reduce disulfide bonds and then alkylated the liberated thiols and any other cysteine residues with IAA. Analysis of the reduced sample by nanoLC-MS/MS (data not shown) revealed a peptide monoisotopic mass of 4028.708 Da (Table 1). The 6.047 Da shift in peptide monoisotopic mass, which corresponds to the addition of six hydrogen atoms (1.0078 Da each), supported the presence of three disulfide bonds. The sample containing alkylated *Hoa*-D1 (Fig. 1D) yielded an MS spectrum dominated by the +5 charge state (Fig. 1E) at *m/z* 875.174, giving a monoisotopic mass of 4370.837 Da (Table 1). The mass shift from the native peptide, 348.177 Da, results from the carbamidomethylation of six thiol groups. Cumulatively, these data showed that *Hoa*-D1 contained a total of six cysteine residues and three disulfide bonds. When the $[M+5H]^{5+}$ ion for reduced, alkylated *Hoa*-D1 was subjected to CID using the same collision energy (20 eV) used to dissociate the native peptide with disulfide bonds, the resulting MS/MS spectrum yielded many more product ions (Fig. 2B), providing information that could be used to establish the peptide sequence.

To apply *de novo* strategies to sequence reduced, alkylated *Hoa*-D1, we first conducted CID experiments targeting both the +5 and +4 charge states of the ionized *Hoa*-D1; in these experiments, we varied the collision energy to determine optimal conditions for *de novo* sequencing. We found that dissociation of the +5 charge state using a lower collision energy (10 eV) provided better signal intensities for shorter, singly-charged y-series ions (Fig. 3B), while higher collision energies (15–20 eV) provided the most complete series of y- and complementary b-type ions (Fig. 3C and D).

At the lower collision energy (10 eV) and using the analysis of singly-charged, y-type ions, we detected a series of y-type ions (y_1-y_9; Fig. 3B), which established the C-terminal sequence as $VC^*C^*RSGGGY$amide (C^* represents a carbamidomethylated cysteine residue). We were also able to detect a series of b-type ions (b_2-b_6; Fig. 3B), which established the N-terminal sequence as [SY]VRSC^*. Using a higher collision energy of 20 eV (Fig. 2B) and subjecting the MS/MS spectrum to deconvolution (calculation to convert multiply-charged ions to their singly-charged *m/z* values), an almost complete set of y-series ions was detected (Fig. 3B, C and D). Some elements of the sequence that were not revealed by y-series ions, including the sequence gaps from missing y_{33} and y_{28}, were resolved by the detection of b-series ions (b_6 and b_{11}, respectively). Thus, the MS/MS data yielded a complete peptide sequence, with the only ambiguity being the assignment of the identity of [I/L] (isoleucine or leucine), which are two isobaric amino acids that cannot be distinguished by the lower collision energies accessed by the instrumentation used in this study.

To provide further support for the assigned sequence, *Hoa*-D1 was purified using HPLC fractionation and the reduced, alkylated peptide was digested with trypsin and analyzed by chip-based nanoLC-QTOF-MS/MS. This analysis resulted in the detection of five predicted tryptic peptides (Fig. 4A and Table 2). Three of the tryptic peptides (*Hoa*-D1[1–4], [31–34], and [35–39]) eluted early in the chromatogram and *Hoa*-D1[35–39] was detected only as the singly-charged peptide. *Hoa*-D1[5–16] and [17–30] were more strongly retained and yielded more abundant signals. The MS/MS spectrum for each peptide (Fig. 4B–F) provided further confirmation of the amino acid sequence that was predicted by the top-down, *de novo* sequencing.

3.3. In silico identification and predicted post-translational processing of Hoa-D1 precursors

In an attempt to identify the precursor protein from which *Hoa*-D1 is derived, unambiguously determine isoleucine/leucine assignments in the sequence, and predict potential post-translational modifications, the extant *H. americanus* EST and TSA data present in GenBank were searched for transcripts encoding the peptide; the sequence SYVRSCS-SNGGDCVYRCYGNIINGACSGSRVCCRSGGGYG, a putative immature version of the peptide, was used as the BLAST input query for searches of both the EST and TSA datasets. While no TSA sequences were found to encode *Hoa*-D1, four ESTs were identified as encoding it, or a highly similar peptide. Alignment of the deduced *H. americanus Hoa*-D1 precursors is shown in Fig. 5A. As can be seen from this, two of the ESTs (Accession Nos. DV773530 and DV772562; (Stepanyan et al., 2006) encode an identical 63 amino acid prehormone that includes the query sequence. A third EST (Accession No. DV773412; (Stepanyan et al., 2006) encoding a 60 amino acid C-terminal partial precursor also includes the query sequence; the extant portion of this partial protein includes a single substituted amino acid relative to the protein deduced from DV773530 and DV772562, namely a glutamine for lysine substitution at position four of the full-length protein (Fig. 5A). The fourth

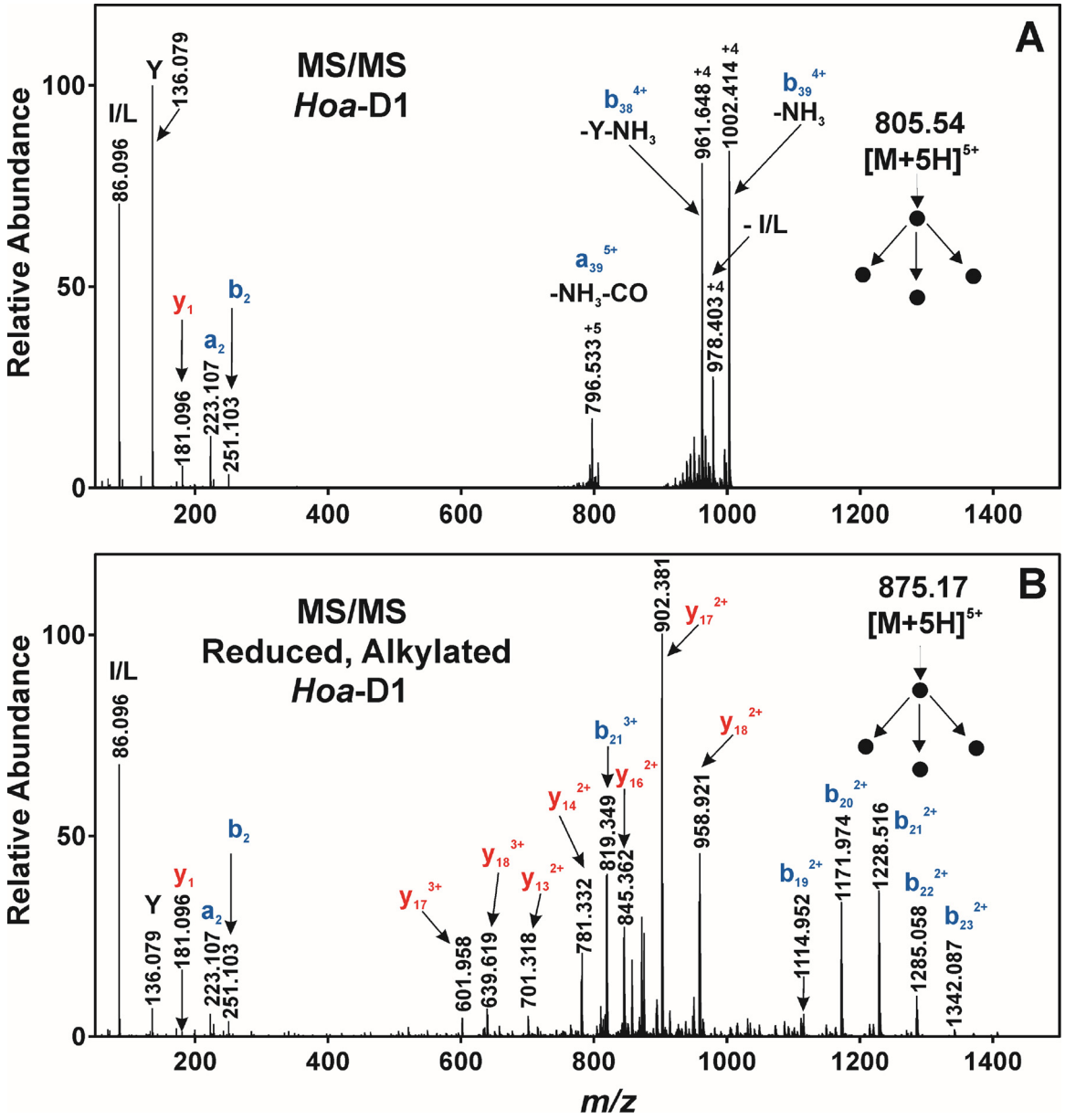

Fig. 2. (A) MS/MS spectrum for the $[M+5H]^{5+}$ charge state of intact *Hoa*-D1 at a collision energy of 20 eV; few informative fragment ions are detected, suggesting that the presence of disulfide bonds have reduced the fragmentation efficiency; (B) MS/MS spectrum for the $[M+5H]^{5+}$ charge state of reduced, alkylated *Hoa*-D1 (*m/z* 875.17) at a collision energy of 20 eV, showing the enhanced number of structurally informative ions relative to the intact *Hoa*-D1 with three disulfide bonds. Monoisotopic masses and charge states are displayed; some fragment ions are identified based upon the detailed sequencing summarized in Fig. 3.

Table 1
Mass measurements for *Hoa*-D1 from heat-treated *H. amerianus* hemolymph, detected as the intact, reduced, and reduced and alkylated forms.

Identity	Measured mass (Da)[a]	Mass Shift (Da)[b]
Hoa-D1	4022.6602	–
Hoa-D1, reduced	4028.7075	6.047
Hoa-D1, reduced and alkylated	4370.8374	348.177

[a] Monoisotopic mass determined following resolved isotope deconvolution.
[b] Mass difference relative to *Hoa*-D1.

EST (Accession No. GO271346; Verslycke et al., unpublished GenBank submission) encodes a 63 amino acid full-length protein that differs from that derived from DV773530 and DV772562 only in an arginine for cysteine substitution at position 55 (Fig. 5A). The hypothetical processing of the prepro-*Hoa*-D1 deduced from ESTs DV773530 and DV772562 is shown in Fig. 5B. The sequence of the final mature peptide is predicted to be SYVRSCSSNGGDCVYRCYGNIINGACSGSRVCCRSG-GGYamide.

Analysis of the nonamidated sequence using two disulfide bond prediction programs, "DiANNA" (http://clavius.bc.edu/~clotelab/DiANNA/; (Ferre and Clote, 2005)) and "DISULFID" (http://disulfind.dsi.unifi.it/; (Ceroni et al., 2006)), both predicted the presence of three disulfide bonds; however, the predicted connectivity (Cys_1-Cys_6, Cys_2-Cys_5, Cys_3-Cys_4 and Cys_1-Cys_4, Cys_2-Cys_5, Cys_3-Cys_6, respectively) differed and, as discussed in more detail below, neither was aligned with predictions for similar peptides. Except for the exact pattern of disulfide bridging, the structure predicted from ESTs DV773530 and DV772562 is identical to that determined via mass spectrometry and resolves the ambiguity of the isobaric leucine/isoleucine residues as two isoleucines. The structure of the putative mature peptide derived from the partial precursor deduced from DV773412 is predicted be identical to that

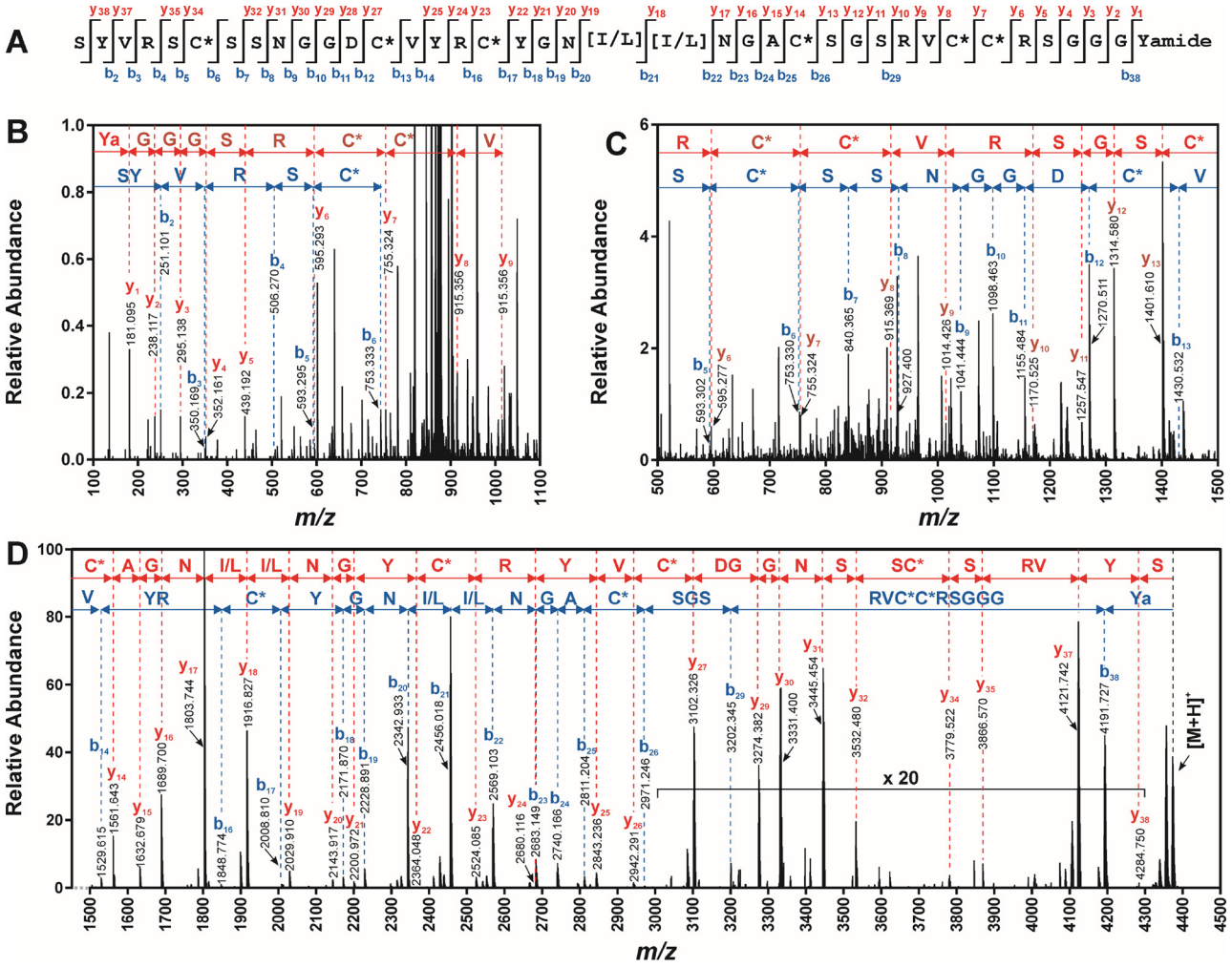

Fig. 3. (A) Amino acid sequence and detected y- and b-type ions for reduced, alkylated *Hoa*-D1 deduced from MS/MS experiments using different collision energies; (B) MS/MS spectrum for the $[M+5H]^{5+}$ charge state of reduced, alkylated *Hoa*-D1 (*m/z* 875.17) at a collision energy of 10 eV, a collision energy that yielded more abundant y- and b-series ions used to establish the C- and N-terminal amino acid sequences; (C and D) Deconvoluted (charge stripped) MS/MS spectra for the $[M+5H]^{5+}$ charge state of reduced, alkylated *Hoa*-D1 (*m/z* 875.17) at a collision energy of 20 eV used to establish the amino acid sequence summarized in (A). Monoisotopic masses for the singly-charged ions are displayed. (C) Expansion of the mass range from *m/z* 500–1500; (D) Expansion of the mass range from *m/z* 1500–4500. "C*" represents a carbamidomethylated cysteine residue; "a" represents amidation.

derived from DV773530 and DV772562, while the arginine for cysteine substitution seen in the protein predicted from GO271346 would result in a putative defensin possessing two rather than three disulfide bonds.

3.4. *Hoa-D1 is a β-defensin-like peptide related to panusin*

BLASTP analysis of the *Hoa*-D1 precursor sequence, searched against non-redundant protein sequences and using default search settings, yielded alignment with three peptides identified as β-defensin-like AMPs from *Panulirus argus* (panusin, Pa-D7, and Pa-D3; (Montero-Alejo et al., 2012, 2017)), and one peptide from *Panulirus japonicas*, Pj-D2 (Pisuttharachai et al., 2009) (see Fig. 6A). Compared with the peptides from *P. argus* and *P. japonicas*, the precursor to *Hoa*-D1 is missing the acidic "EPEP" propiece common to the other precursors; however, N-terminal sequencing has demonstrated that this propiece is missing from the mature *P. argus* peptide, panusin, (Montero-Alejo et al., 2017) and is presumably cleaved during processing. Thus, mature *Hoa*-D1 shares the share the same N-terminal amino acids, "SY", with panusin and the other *P. argus* and *P. japonicas* peptides. Like panusin, *Hoa*-D1 has an amidated tyrosine residue at the C-terminus and, with the exception of Pa-D7, which is missing the glycine residue required for conversion to the C-terminal amide, the other *P. argus* and *P. japonicas* peptides would be predicted to share that C-terminal sequence. In common with the other β-defensin-like peptides, *Hoa*-D1 has one acidic residue (^{12}Asp) and four basic residues ($^{4, 16, 30, 34}$Arg), with an estimated net charge of +3. *Hoa*-D1 also shares the highly conserved asparagine (^{9,20}Asn), glycine (^{10,11}Gly), and a single valine (^{14}Val) residue with the other β-defensin-like peptides. In contrast with panusin, Pa-D7 and Pa-D3, the arginine residues in *Hoa*-D1 are not located towards the C-terminus, but are more distributed throughout the sequence, and the single aspartate residue is shifted away from the N-terminus.

When the cysteine spacing patterns of the peptides are compared, *Hoa*-D1, with a C-X_6-C-X_3-C-X_8-C-X_5-C-C pattern, differs only slightly from the pattern exhibited by the other three peptides (C-X_6-C-X_4-C-X_9-C-X_5-C-C for panusin, Pa-D7 and Pa-D3; C-X_6-C-X_4-C-X_7-C-X_5-C-C for Pj-D2), with the *Hoa*-D1 and *P. argus* peptides falling within the C-$X_{4\text{-}8}$-C-$X_{3\text{-}5}$-C-$X_{9\text{-}13}$-C-$X_{4\text{-}7}$-C-C pattern characteristic of β-defensins (Zhao et al., 2016). Regarding disulfide connectivity, the bonding patterns for *Hoa*-D1 and panusin have not been established experimentally. However, the Cys_1-Cys_5, Cys_2-Cys_4, Cys_3-Cys_6 connectivity established for β-defensins (Kluver et al., 2006; Zhao et al., 2016) was successfully applied to structural models for panusin (Montero-Alejo et al., 2017), suggesting that this connectivity may also be expected for *Hoa*-D1.

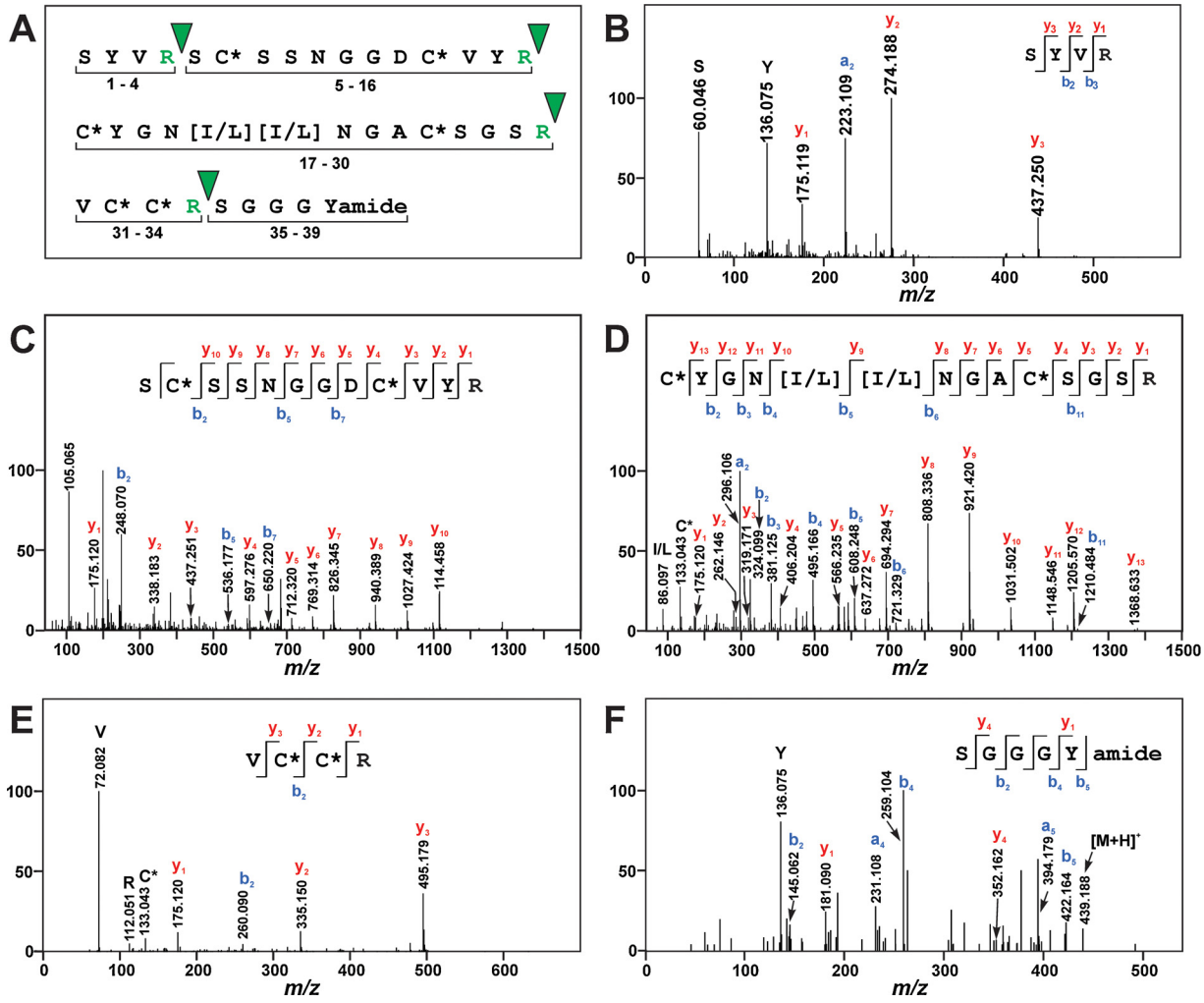

Fig. 4. MS/MS spectra of tryptic peptides detected following reduction, alkylation, and digestion of *Hoa*-D1. (A) Amino acid sequence for reduced, alkylated *Hoa*-D1, showing sites of cleavage by trypsin; (B) MS/MS spectrum for the *m/z* 262.64, $[M+2H]^{2+}$ ion from *Hoa*-D1[1–4]; (C) MS/MS spectrum for the *m/z* 681.26, $[M+2H]^{2+}$ ion from *Hoa*-D1[5–16]; (D) MS/MS spectrum for the *m/z* 764.84, $[M+2H]^{2+}$ ion from *Hoa*-D1[17–30]; (E) MS/MS spectrum for the *m/z* 297.63, $[M+2H]^{2+}$ ion from *Hoa*-D1[31–34]; (F) MS/MS spectrum for the *m/z* 439.19, $[M+H]^{+}$ ion from *Hoa*-D1[35–39]."C*" represents a carbamidomethylated cysteine residue.

Table 2
Mass measurements for tryptic peptides from *Hoa*-D1.

Sequence[a]	Start[b]	End[c]	Measured mass (Da)[d]	Predicted mass (Da)[d]	Error (ppm)[e]
SYVR	1	4	523.2780	523.2754	4.9
SC*SSNGGDC*VYR	5	16	1360.5140	1360.5136	0.3
C*YGN[I/L][I/L]NGAC*SGSR	17	30	1527.6546	1527.6558	−0.8
VC*C*R	31	34	593.2420	593.2414	1.0
SGGGYamide	35	39	438.1880	438.1863	4.0

[a] C* denotes carbamidomethylated cysteine.
[b] Starting amino acid number in the *Hoa*-D1 sequence.
[c] Ending amino acid number in the *Hoa*-D1 sequence.
[d] Monoisotopic mass.
[e] Error(ppm) = $((M_{meaured} - M_{predicted})*10^6/M_{predicted})$

3.5. Disulfide bond linkages were challenging to establish experimentally

The mass spectrometric assignment of disulfide bond linkages for peptides like *Hoa*-D1 with three internal disulfide bonds and adjacent cysteine residues ($^{32}Cys_5$ and $^{33}Cys_6$, for *Hoa*-D1) presents challenges because of the number of possible connections, the difficulty associated with distinguishing bonds to the adjacent cysteine residues, and the possibility of disulfide bond scrambling (Tsai et al., 2013). In our study, we undertook two, ultimately unsuccessful, experimental approaches, i.e., partial disulfide bond reduction and enzymatic digestion (described in Supplemental Data), in attempts to establish connectivity. Our attempts to partially reduce disulfide bonds (data not shown) employed tris(2-carboxyethyl)phosphine (TCEP) as a reducing agent that is effective under the acidic conditions that minimize disulfide bond

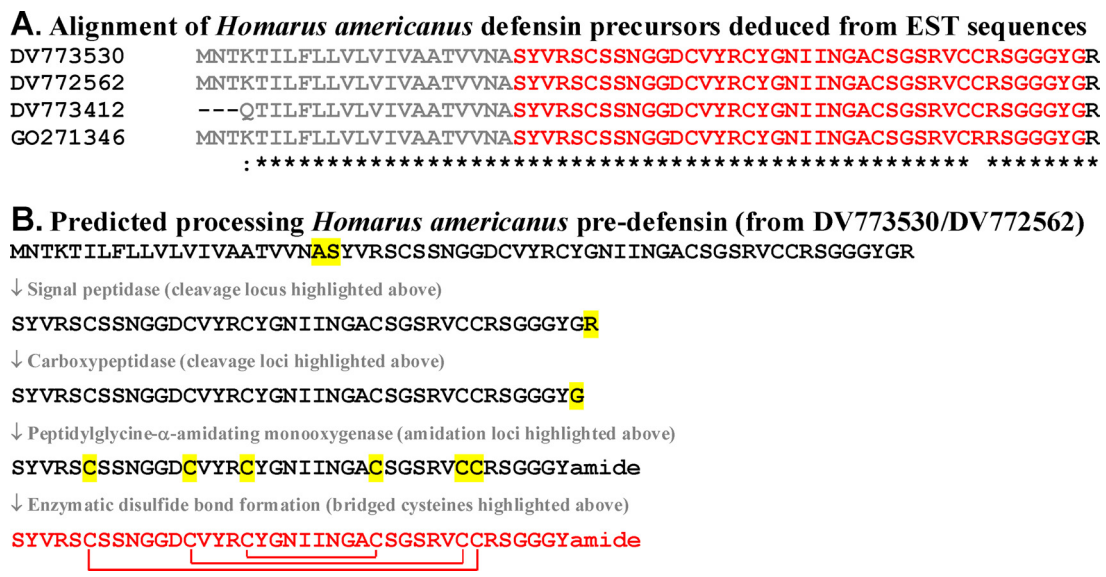

Fig. 5. *In silico* identification and predicted post-translational processing of putative *Homarus americanus Hoa*-D1 precursors. (**A**) Alignment of putative pre-*Hoa*-D1 deduced from expressed sequence tags (ESTs). EST accession numbers are shown on the left, with amino acid sequences of the peptides deduced from them shown on the right. In this alignment, putative signal peptides have been colored gray, with the putative *Hoa*-D1 in each precursor colored red. In the line immediately below the grouping, "*" indicates identical amino acid residues, while ":" denotes amino acids that are similar in structure between the sequences. (**B**) Putative processing scheme of the *Hoa*-D1 prehormone deduced from DV773530 and DV772562. In this panel, the sequence of the putative mature defensin is shown in red; lower case "c" represents a cysteine residue that participates in a disulfide bond. (For interpretation of the references to colour in this figure legend, the reader is referred to the web version of this article.)

scrambling. We reacted purified *Hoa*-D1 with TCEP, and varied both concentrations and reaction times with the goal of generating the partially reduced peptide. Our attempts resulted in either complete reduction or the generation of multiple, low-abundance products that showed evidence for disulfide bond scrambling and deamidation, as determined by chromatographic retention and an evaluation of MS and MS/MS spectra (data not shown), which made disulfide bond assignments unreliable. We also attempted the enzymatic digestion of intact *Hoa*-D1 using trypsin at pH = 7.0, an approach employed in other studies to characterize disulfide bonding in structurally related AMPs (Hung et al., 2014; Tang and Selsted, 1993). We found *Hoa*-D1 to be resistant to complete digestion, with cleavages limited to the arginine residues close to the N- and C-terminus (^{4}Arg and ^{34}Arg) and no evidence for enzymatic cleavage at the two residues (^{16}Arg and ^{30}Arg) located within the disulfide bonded motif, even after digesting for longer times (3 days) and following additions of fresh trypsin.

3.6. Hoa-D1 is likely CAP-1, which was isolated and partially sequenced from H. americanus hemocytes

In an earlier study by Battison and co-workers (Battison et al., 2008), two peptides, CAP-1 and CAP-2, were isolated from *H. americanus* hemocyte extracts and partially characterized by digestion and mass spectrometric analysis. CAP-2, with an SDS-PAGE gel-assigned molecular mass of ~12-kDa, was identified as *Hoa*-crustin. CAP-1, with an SDS-PAGE gel-assigned molecular mass in the range of 4-6-kDa, was not definitively identified. Four tryptic fragments were detected, partially sequenced, and found to show homology with temporins (Battison et al., 2008). While mass spectral data and digestion protocols, including the alkylating agent employed, were not provided in the publication, the reported *de novo* sequenced tryptic fragments showed homology to the sequence we determined for *Hoa*-D1. Specifically, a tryptic fragment with the sequence "XXSSNGGDCVYR", with XX potentially equal to "SC" was reported (Battison et al., 2008). This sequence is identical to the *Hoa*-D1[5–16] fragment identified in our study and provides evidence to connect *Hoa*-D1 to CAP-1. The peptide CAP-1 exhibited protozoastatic or protozoacidal activity against ciliate parasites, including the parasite *Anophryoides haemophila*, which causes bumper car disease in the lobster (Battison et al., 2008); the peptide also exhibited selective bacteriostatic activity against Gram negative organisms. This connection suggests that *Hoa*-D1 is likely to serve as an antimicrobial agent in *H. americanus*.

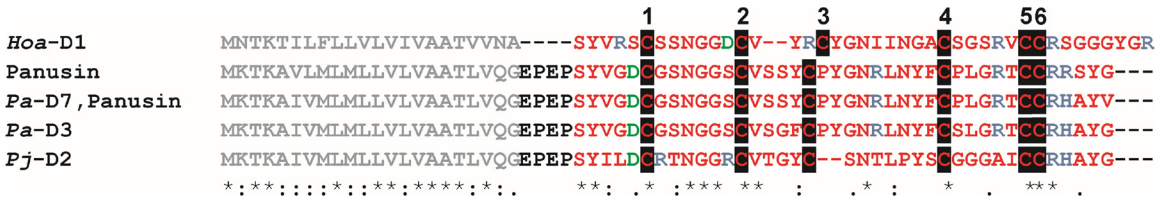

Fig. 6. Alignment of the translated *Hoa*-D1 precursor with peptides with significant alignment from the NCBI non-redundant protein database: Panusin (AC: ALQ10737.1); Pa-D7, Panusin (AC: F6KSI8.10); Pa-D3 (AC: AEE69604.1); Pj-D2 (AC: ACM62358.1). In the line immediately below the grouping, "*" indicates identical amino acid residues, while ":" and "." denote amino acids that are similar in structure between the sequences. Putative signal peptides have been colored gray, the acidic propiece is colored black; the putative *Hoa*-D1 in each precursor is colored red; cysteine residues are highlighted in black; acidic amino acid residues are colored in green; basic residues are colored in blue. (For interpretation of the references to colour in this figure legend, the reader is referred to the web version of this article.)

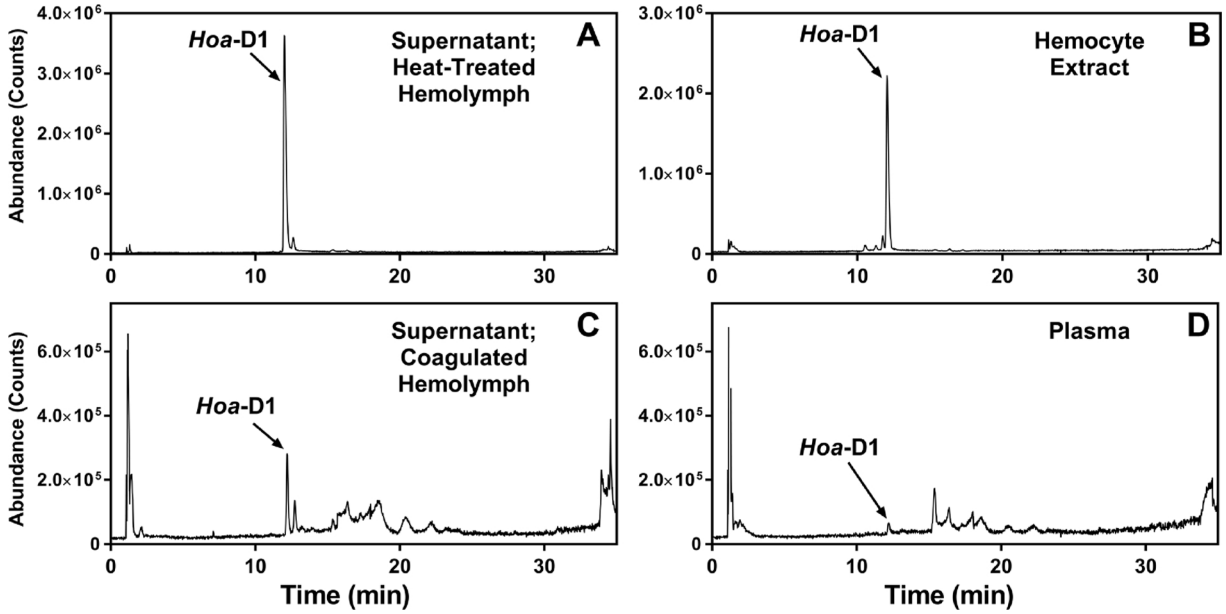

Fig. 7. LC/MS chromatograms (m/z 450–2000) for (A) supernatant isolated from heat-treated hemolymph after centrifugation; 0.1 µL injection from ~ 400 µL of supernatant; (B) extract from hemocytes separated from hemolymph treated with anticoagulant after centrifugation; 0.1 µL injection from ~ 400 µL of extract; (C) supernatant isolated from coagulated hemolymph after centrifugation; 0.1 µL injection from ~ 200 µL of supernatant; (D) plasma separated from hemolymph treated with anticoagulant after centrifugation; 1.0 µL injection from ~ 1000 µL of supernatant. All samples prepared from 500 µL hemolymph; higher molecular mass components were removed using 30-kDa MWCO filters prior to analysis.

3.7. Hoa-D1 is detected in heat-treated hemolymph, mixed hemocyte extracts, and some plasma samples

Hoa-D1 was initially identified using the supernatant from *H. americanus* hemolymph samples that were heat-treated prior to analysis. To determine if *Hoa*-D1 was present in hemocyte extracts and hemolymph plasma, hemolymph samples (drawn from the same individual) were subjected to heat-treatment or were mixed with anticoagulant and centrifuged to separate intact hemocytes and plasma; the isolated hemocytes were then lysed and extracted. Higher molecular mass proteins were removed from all samples using 30-kDa MWCO filters and the samples were analyzed by nanoLC-MS/MS, with representative results shown in Fig. 7.

Hoa-D1 was consistently found as an abundant peak for all heat-treated hemolymph samples and for hemocyte extracts (representative data shown in Fig. 7A and B). *Hoa*-D1 was also detected in the serum from coagulated hemolymph (Fig. 7C) and in four of five plasma samples (Fig. 7D). However, signal intensities for *Hoa*-D1 were always approximately ten times lower in serum or plasma compared with the signals from samples derived from an equivalent volume of heat-treated hemolymph. These results support the expectation that *Hoa*-D1 is synthesized in *H. americanus* hemocytes. The peak areas for *Hoa*-D1 from heat-treated hemolymph and hemocyte extracts, for samples derived from an equivalent volume of hemolymph, were similar in magnitude, suggesting that *Hoa*-D1 is efficiently released and isolated from hemocytes upon heat-treatment. Our detection of a lower abundance *Hoa*-D1 peak in some plasma samples supports the hypothesis that *Hoa*-D1 is released from hemocytes into the circulatory fluid, again suggesting that it may function as a circulating AMP in *H. americanus*.

3.8. Hoa-D1 is detected in extracts from cells identified as granulocytes and semigranulocytes

To explore further the localization of *Hoa*-D1, *H. americanus* hemocytes were separated into sub-populations using a Percoll discontinuous density gradient separation. Following centrifugation, three fractions were observed as layers separated from the plasma and cellular debris (Fig. 8A). Cellular identify was assigned based upon the location of the cells in the gradient and by morphological characteristics. Cells in the top fraction (F-1), which formed at the interface of the 30% and 60% Percoll solutions, were identified as being primarily hyalinocytes based upon their smaller size (Fig. 8B). Cells in the middle fraction (F-2), which formed at the interface of the 60% and 80% Percoll solutions, were identified as being primarily semigranulocytes, based upon the observation of cells with an oval appearance and larger size (Fig. 8C). Cells in the bottom fraction (F-3), which formed at the bottom of the 80% Percoll solution, were identified as primarily granulocytes, based upon their spherical shapes and larger sizes (Fig. 8D).

To localize *Hoa*-D1 to the fractionated cells, cell lysates from each of the cell fractions were subjected to analysis by (1) SDS-PAGE with in-gel digestion of excised bands and (2) nanoLC-MS/MS analysis of intact peptides from lysates following removal of larger proteins with 30-kDa MWCO filters. SDS-PAGE analysis of mixed and fractionated hemocytes lysates from two individuals (Fig. 9) revealed distinct profiles for the three hemocyte sub-populations. Relevant to this study is the observation of a band appearing near the 5-kDa MW ladder marker in lanes for the mixed hemocytes (HCs; Fig. 9), semigranulocytes (SG; F-2; Fig. 9), and granulocytes (G; F-3; Fig. 9). We hypothesized that this band contained *Hoa*-D1, with the diffuse appearance of the band showing behavior similar to that observed in previous work (Battison et al., 2008). We confirmed that *Hoa*-D1 was present in this band by excising this region from the gel for all eight samples and subjecting each sample to in-gel digestion and proteomic analysis. NanoLC–MS/MS analysis of the extracted tryptic peptides found *Hoa*-D1-derived peptides in digests from the mixed hemocyte, semigranulocyte, and granulocyte bands (Table 3). Weak signals for two *Hoa*-D1 tryptic peptides were detected in the hyalinocyte band digest from one individual (Lobster A; Table 3); we hypothesize that these signals may result from some cell mixing that occurred during hemocyte fractionation.

NanoLC–MS/MS was used as a complementary approach to localize *Hoa*-D1 to sub-populations of hemocytes via the analysis of intact peptides from hemocyte extracts following the removal of higher molecular mass proteins using 30-kDa MWCO filters. While low intensity signals corresponding to *Hoa*-D1 were detected in extracts from

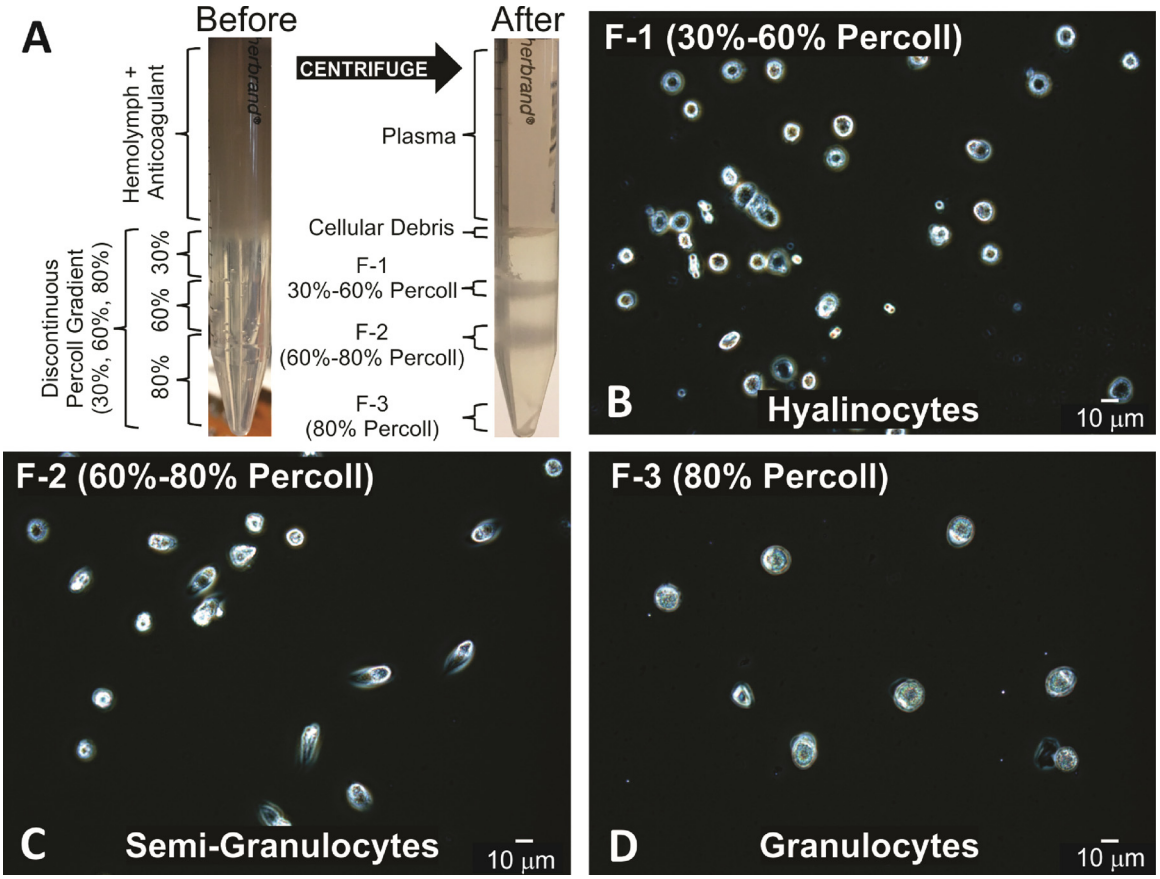

Fig. 8. Mixed hemocytes from *H. americanus* hemolymph were separated into three morphologically distinct sub-populations using a discontinuous Percoll gradient. (A) Hemolymph mixed with anticoagulant was layered and separated in a discontinuous density gradient of 30%, 60%, and 80% Percoll resulting in separation into plasma, cellular debris and three visible fractions. (B–D) Separated fractions were visualized via bright-field microscopy. (B) Fraction 1, removed from the 30–60% Percoll border, primarily contained hemocytes identified as hyalinocytes (HY; diameter = ~5 µm); (C) Fraction 2, removed from the 60%–80% Percoll border, primarily contained hemocytes identified as semigranulocytes (SG); and (D) Fraction 3, removed from 80% Percoll, primarily contained hemocytes identified as granulocytes (G; diameter = ~15 µm.)

hyalinocytes (Fig. 10A and E), strong *Hoa*-D1 signals were detected in extracts from the semigranulocytes (Fig. 10B and F). These results aligned with data from the SDS-PAGE analyses, where the semigranulocytes showed an intense ~5 kDa band that in-gel digestion showed contained *Hoa*-D1. As described above, we hypothesize that the weak signals for *Hoa*-D1 for the hyalinocytes may result from cellular contamination.

In contrast with the signals observed for the semigranulocytes, where *Hoa*-D1 represented > 95% of the area for peptides detected by direct LC/MS analysis, *Hoa*-D1 was found as a lower abundance component when the granulocytes extracts were subjected to direct LC/MS analysis (Fig. 10C and G). Furthermore, the *Hoa*-D1 peak was accompanied by a collection of more abundant, earlier-eluting peaks. A detailed examination of these peaks revealed three dominant components (*I, II, III*; Fig. 10D and H and Table 4). We identified peptides *II* and *III* as C-terminally truncated versions of *Hoa*-D1, in which the peptide has lost the C-terminal tyrosine residue, based upon exact mass measurements (Table 4) and MS/MS spectra (Figs. S1 and S2, Supplemental Data). The MS data supported the identification of the later-eluting peptide (*III*) as truncated *Hoa*-D1 with a C-terminal acid, not amide, group (Table 4); the earlier-eluting peptide (*II*) was identified as the truncated peptide, but with a C-terminal amide group (Table 4). The earliest-eluting peptide (*I*; 4145.68 Da) yielded an MS/MS spectrum (Fig. S3, Supplemental Data) indicating that the peptide was a structurally altered form of *Hoa*-D1, based upon the detection of b-series ions (b_2, b_3, and b_4) and the more limited overall degree of fragmentation, reflecting the presence of disulfide bonds. The highest detected charge state for peptide *I* (+6) was higher than that detected for *Hoa*-D1 (+5), which suggests that the peptide has been altered by the addition of a new basic site that would accommodate an additional proton. We have not structurally characterized peptide *I*; however, the detection of these three altered forms of *Hoa*-D1 suggests that *Hoa*-D1 may undergo endogenous enzymatic degradation or processing in a manner that is specific to granulocytes; alternatively, conversion of *Hoa*-D1 to these three modified forms could have occurred during hemocyte extraction.

Our detection of modified forms of *Hoa*-D1 via the analysis of the intact peptides is consistent with our detection of tryptic peptides derived from unmodified *Hoa*-D1 because the MS evidence suggests that the modifications were located at the C-terminus of *Hoa*-D1. Thus, the tryptic peptides containing the N-terminus and all internal fragments would remain unchanged and the modifications would only be revealed by detection of modified forms of the tryptic peptide containing the C-terminus. For unmodified *Hoa*-D1, this tryptic peptide (*Hoa*-D1[35–39]) has been more challenging to detect because it contains no basic residues and elutes earlier in the chromatogram; if truncated or modified, the peptide would not be identified using conventional proteomic database searching strategies because, even if it was detected, the mass and sequencing would not align with the database predictions. When we specifically examined the data to find the C-terminally modified tryptic fragments from the in-gel digested granulocyte samples, they were not detected; however, we would expect them to elute even earlier than *Hoa*-D1[35–39], as would be predicted by the elution pattern of intact peptides *I, II, and III* relative to *Hoa*-D1, and detection would be less likely.

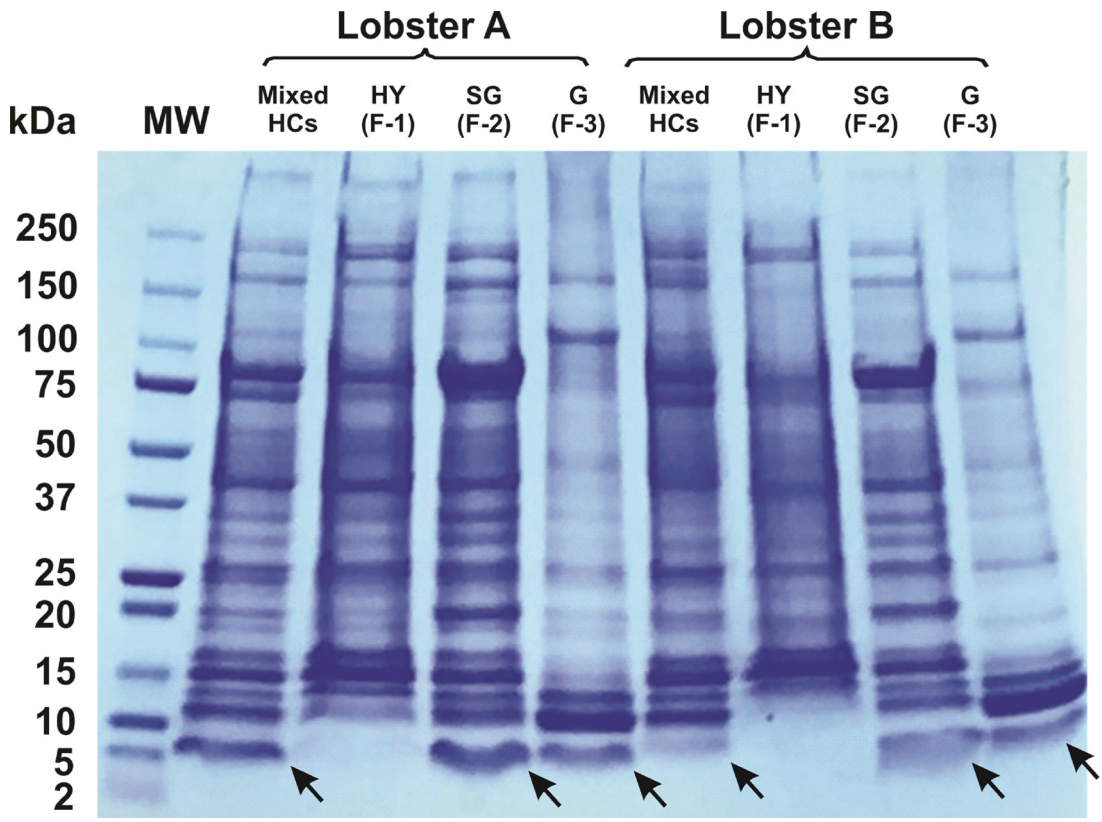

Fig. 9. SDS-PAGE (4%-gradient 20%) fixed with Coomassie blue protein staining of cell lysates from mixed and fractionated *H. americanus* hemocytes, showing evidence for a band, indicated by arrows, consistent with the MW of *Hoa*-D1 (~4 kDa). *Hoa*-D1-assigned bands were observed for lysates from mixed hemocytes (HCs) and two hemocyte fractions: F-2 (60–80% Percoll), cells identified as primarily semigranulocytes (SGs), and F-3 (80% Percoll), cells identified as primarily granulocytes. No band was observed for F-1 (30%–60% Percoll), cells identified as primarily hyalinocytes. Two individuals (Lobster A, female; Lobster B, male) were analyzed; 30 µg of protein loaded for each lane. (For interpretation of the references to colour in this figure legend, the reader is referred to the web version of this article.)

Table 3
Tryptic peptides detected by nanoLC-MS/MS following the in-gel digestion of the excised ~5 kDa bands shown in Fig. 9.

Sequence[a]	Percoll Fraction[b] Lobster A			Percoll Fraction[b] Lobster B		
	F-1[c]	F-2	F-3	F-1[c]	F-2	F-3
SYVR; *Hoa*-D1 [1-4]	–	+	+	–	+	+
SC*SSNGGDC*VYR; *Hoa*-D1 [5-16]	–	+	+	–	+	+
SYVRSC*SSNGGDC*VYR; *Hoa*-D1 [1-16][d]	–	+	+	–	+	+
C*YGNIINGAC*SGSR; *Hoa*-D1 [17-30]	–	+	+	+	+	+
VC*C*R; *Hoa*-D1 [31-34]	–	–	–	–	–	–
SGGGYamide; *Hoa*-D1 [35-39]	–	+	–	–	–	–

[a] Sequence and starting to ending amino acid number in the *Hoa*-D1 sequence; C* denotes carbamidomethylated cysteine.
[b] Sample from which the ~5 kDa gel band was excised (see Fig. 9).
[c] Although no visible band was detected, an equivalent area of the gel was excised and subjected to in-gel digestion.
[d] Tryptic peptide with one missed cleavage.

In summary, the direct nanoLC-MS/MS analysis of extracts from fractionated hemocytes showed strong signals for *Hoa*-D1 for the semigranulocytes, which was consistent with the detection of the peptide via proteomic analysis of the SDS-PAGE-separated bands, while *Hoa*-D1 signals from the hyalinocyte extracts were of low intensity, again showing good agreement with the SDS-PAGE and proteomic analysis. In contrast, the direct analysis of granulocyte extracts provided evidence that C-terminally modified forms of *Hoa*-D1 were present, information that was consistent with the SDS-PAGE analysis and proteomic analysis with detection of N-terminal and internal tryptic peptides; however, this analysis revealed new information about modifications that would only be apparent from the analysis of the undigested peptides.

3.9. *Hoa-D1 is detected in extracts from H. americanus neural tissues*

When *H. americanus* neural tissues (brain, eyestalk ganglia, and PO) were extracted and analyzed by nanoLC-MS/MS, *Hoa*-D1 was consistently detected in all analyzed samples ($n > 3$ for each tissue type; see Figs. S4–7, Supplemental Data and Table 5). A single peak for *Hoa*-D1 was detected in the nanoLC-MS/MS analysis of eyestalk ganglia (Fig. S4), PO (Fig. S5), and 10 of 16 supraoesophageal ganglion (brain; Fig. S6) tissue extracts; in the remaining six brain samples (see Fig. S7), a collection of later eluting peaks, all exhibiting MS spectra characteristic

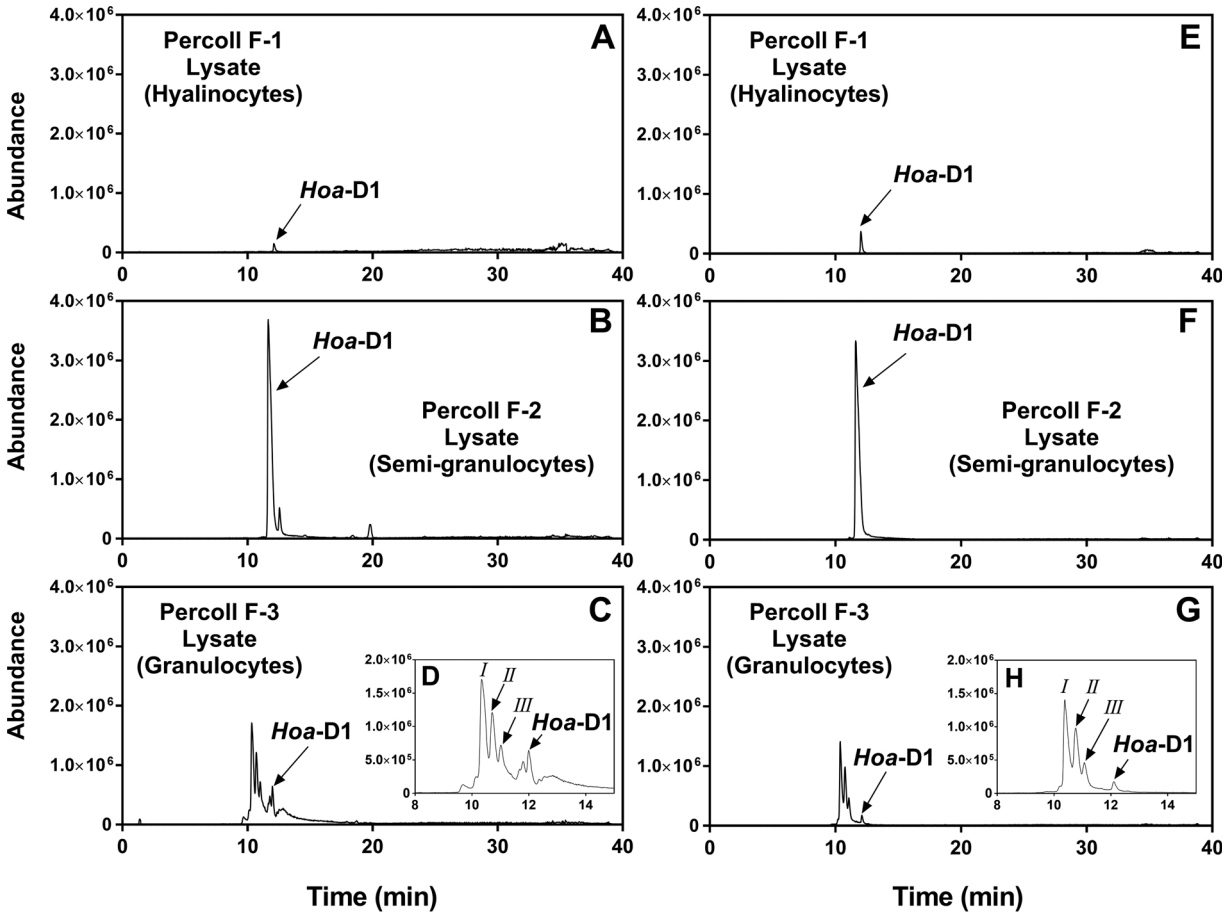

Fig. 10. LC/MS chromatograms (*m/z* 450–2000) for lysates extracted from sub-populations of *H.americanus* hemocytes, separated by Percoll density centrifugation; hemocytes collected from two individuals (A and E) Lysate from fraction F-1 (30%–60% Percoll); cells identified as primarily hyalinocytes. Percoll supernatant isolated from heat-treated hemolymph after centrifugation; 0.1 µL injection from ~ 400 µL of supernatant; (B) extract from hemocytes separated from hemolymph treated with anticoagulant after centrifugation; 0.1 µL injection from ~ 400 µL of extract; (C) supernatant isolated from coagulated hemolymph after centrifugation; 0.1 µL injection from ~ 200 µL of supernatant; (D) plasma separated from hemolymph treated with anticoagulant after centrifugation; 1.0 µL injection from ~ 1000 µL of supernatant. All samples prepared from 500 µL hemolymph; higher molecular mass components were removed using 30-kDa MWCO filters prior to analysis.

of *Hoa*-D1, were detected. The MS/MS spectra for these components yielded peaks characteristic of *Hoa*-D1; however, the spectra were distinctly different in terms of product ion abundances, suggesting that these peptides corresponded to forms of *Hoa*-D1 that had undergone disulfide bond scrambling/isomerization. The shifts to later elution times could be attributed to changes in peptide shape and hydrophobicity, which could be associated with changes in disulfide bond connectivity. Upon reduction and alkylation, the collection of 4022.66 Da peptides was converted to a single peak at 4370.84 Da, providing further support for this hypothesis. At this point, it is unclear if the putative disulfide bond scrambling is a biological modification or is a chemical artifact from our tissue extraction procedure.

4. Conclusions

We report, for the first time, on the detection of the mature form of a β-defensin-like peptide, *Hoa*-D1, in the hemocytes, hemolymph, and neural tissues from the lobster, *H. americanus*, using a sensitive chip-based nanoLC-QTOF-MS/MS method of analysis. This peptide, homologous to peptides from *P. japonicas* and *P. argus*, was detected with

Table 4
Sequences and exact mass measurements for modified forms of *Hoa*-D1 detected in the analysis of intact peptides from *H. americanus* F-3 (granulocyte) extracts.

Peptide name and sequence[a]	Measured mass (Da)[b]	Predicted mass (Da)[b]	Error (ppm)[c]
Peptide I	4145.6750	–[d]	–[d]
Hoa-D1-derived peptide[d]			
Peptide II	3859.5980	3859.5912	1.8
SYVRScSSNGGDcVYRcYGNIINGAcSGSRVccRSGGGamide			
Peptide III	3860.5807	3860.5753	1.4
SYVRScSSNGGDcVYRcYGNIINGAcSGSRVccRSGGG			

[a] "c" represents a cysteine residue participating in a disulfide bond.
[b] Monoisotopic mass.
[c] Error(ppm) = $((M_{meaured}-M_{predicted})*10^6/M_{predicted})$.
[d] Peptide identity has not been established.

Table 5
Exact mass measurements for *Hoa*-D1 detected in *H. americanus tissue extracts*.

Tissue	Measured mass (Da)[b]	Predicted mass (Da)[a]	Error (ppm)[b]
Supraoesophageal ganglion (brain)yptic peptides detected by nanoLC-MS/MS following the in-gel digestion of t	4022.6621	4022.6545	1.9
Eyestalk ganglia	4022.6642	4022.6545	2.4
Pericardial organs	4022.6672	4022.6545	3.2

[a] Monoisotopic mass.
[b] Error(ppm) = $((M_{meaured}-M_{predicted})*10^6/M_{predicted})$.

three disulfide-bonds and an amidated C-terminus as post-translational modifications. Fractionation of mixed hemocytes using discontinuous density centrifugation and analysis of the separated hyalinocytes, semigranulocytes, and granulocytes by SDS-PAGE with in-gel digestion and the direct LC/MS analysis of hemocyte extracts showed that *Hoa*-D1 is clearly localized to the semigranulocytes. While *Hoa*-D1 was detected in the granulocytes, the direct analysis of granulocyte extracts provided evidence for the conversion of *Hoa*-D1 to three modified forms, two of which were C-terminally truncated forms of *Hoa*-D1, a result that emphasizes the need to structurally characterize putative AMPs, like *Hoa*-D1, using techniques that interrogate the intact peptide and reveal peptide modifications. Work is needed to explore the functional roles of *Hoa*-D1 and determine if the observed processing of *Hoa*-D1 plays a role in the degradation or activation of *Hoa*-D1.

Declaration of interests

The authors have no conflicts of interest to declare.

Acknowledgements

This work was supported by funding from the National Science Foundation [IOS-1354567 to PSD; IOS-1353023 to AEC; CHE-1126657 to EAS] and an Institutional Development Award (IDeA) from the National Institute of General Medical Sciences of the National Institutes of Health [grant number P20GM0103423]. Funding was also provided by Bowdoin College. We thank Julia Michels and Peter Tracy for their assistance with the collection and nanoLC-MS analysis of extracted brain and eyestalk ganglia tissues.

Appendix A. Supplementary data

Supplementary material related to this article can be found, in the online version, at doi:https://doi.org/10.1016/j.molimm.2018.07.004.

References

Afsal, V.V., Antony, S.P., Bright, A.R., Philip, R., 2013. Molecular identification and characterization of type I crustin isoforms from the hemocytes of portunid crabs, *Scylla tranquebarica* and *Portunus pelagicus*. Cell. Immunol. 284, 45–50.
Antony, S.P., Singh, I.S.B., Sudheer, N.S., Vrinda, S., Priyaja, P., Philip, R., 2011. Molecular characterization of a crustin-like antimicrobial peptide in the giant tiger shrimp, *Penaeus monodon*, and its expression profile in response to various immunostimulants and challenge with WSSV. Immunobiology 216, 184–194.
Balandin, S.V., Ovchinnikova, T.V., 2016. Antimicrobial peptides of invertebrates. Part 1. Structure, biosynthesis, and evolution. Russ. J. Bioorg. Chem. 42, 229–248.
Battison, A.L., Summerfield, R., Patrzykat, A., 2008. Isolation and characterisation of two antimicrobial peptides from haemocytes of the American lobster Homarus americanus. Fish Shellfish Immunol. 25, 181–187.
Beale, K.M., Towle, D.W., Jayasundara, N., Smith, C.M., Shields, J.D., Small, H.J., Greenwood, S.J., 2008. Anti-lipopolysaccharide factors in the American lobster *Homarus americanus*: molecular characterization and transcriptional response to *Vibrio fluvialis* challenge. Comp. Biochem. Physiol. Part D Genomics Proteomics 3D, 263–269.
Cawthorn, R.J., 2011. Diseases of American lobsters (*Homarus americanus*): a review. J. Invertebr. Pathol. 106, 71–78.
Ceroni, A., Passerini, A., Vullo, A., Frasconi, P., 2006. DISULFIND: a disulfide bonding state and cysteine connectivity prediction server. Nucleic Acids Res. 34, W177–W181.
Christie, A.E., 2016a. Expansion of the neuropeptidome of the globally invasive marine crab *Carcinus maenas*. Gen. Comp. Endocrinol. 235, 150–169.
Christie, A.E., 2016b. Prediction of *Scylla olivacea* (Crustacea; Brachyura) peptide hormones using publicly accessible transcriptome shotgun assembly (TSA) sequences. Gen. Comp. Endocrinol. 230–231, 1–16.
Christie, A.E., Pascual, M.G., 2016. Peptidergic signaling in the crab *Cancer borealis*: tapping the power of transcriptomics for neuropeptidome expansion. Gen. Comp. Endocrinol. 237, 53–67.
Christie, A.E., Rus, S., Goiney Christopher, C., Smith Christine, M., Towle David, W., Dickinson Patsy, S., 2007. Identification and characterization of a cDNA encoding a crustin-like, putative antibacterial protein from the American lobster *Homarus americanus*. Mol. Immunol. 44, 3333–3337.
Clark, K.F., Acorn, A.R., Greenwood, S.J., 2013a. Differential expression of American lobster (*Homarus americanus*) immune related genes during infection of *Aerococcus viridans var. homari*, the causative agent of Gaffkemia. J. Invertebr. Pathol. 112, 192–202.
Clark, K.F., Acorn, A.R., Greenwood, S.J., 2013b. A transcriptomic analysis of American lobster (*Homarus americanus*) immune response during infection with the bumper car parasite *Anophryoides haemophila*. Dev. Comp. Immunol. 40, 112–122.
Clark, K.F., Greenwood, S.J., Acorn, A.R., Byrne, P.J., 2013c. Molecular immune response of the American lobster (*Homarus americanus*) to the White spot syndrome virus. J. Invertebr. Pathol. 114, 298–308.
Donpudsa, S., Rimphanitchayakit, V., Tassanakajon, A., Soederhaell, I., Soederhaell, K., 2010. Characterization of two crustin antimicrobial peptides from the freshwater crayfish *Pacifastacus leniusculus*. J. Invertebr. Pathol. 104, 234–238.
Ferre, F., Clote, P., 2005. DiANNA: a web server for disulfide connectivity prediction. Nucleic Acids Res. 33, W230–W232.
Hancock, R.E.W., Brown, K.L., Mookherjee, N., 2006. Host defence peptides from invertebrates - emerging antimicrobial strategies. Immunobiology 211, 315–322.
Hung, C.-W., Jung, S., Grotzinger, J., Gelhaus, C., Leippe, M., Tholey, A., 2014. Determination of disulfide linkages in antimicrobial peptides of the macin family by combination of top-down and bottom-up proteomics. J. Proteomics 103, 216–226.
Kang, H.K., Seo, C.H., Park, Y., 2015. Marine peptides and their anti-infective activities. Mar. Drugs 13, 618–654 637 pp.
Katoh, K., Standley, D.M., 2013. MAFFT multiple sequence alignment software version 7: improvements in performance and usability. Mol. Biol. Evol. 30, 772–780.
Kluver, E., Adermann, K., Schulz, A., 2006. Synthesis and structure-activity relationship of β-defensins, multi-functional peptides of the immune system. J. Pept. Sci. 12, 243–257.
Kumar, D., Bansal, G., Narang, A., Basak, T., Abbas, T., Dash, D., 2016. Integrating transcriptome and proteome profiling: strategies and applications. Proteomics 16, 2533–2544.
Liu, N., Zhang, R.-R., Fan, Z.-X., Zhao, X.-F., Wang, X.-W., Wang, J.-X., 2016. Characterization of a type-I crustin with broad-spectrum antimicrobial activity from red swamp crayfish *Procambarus clarkii*. Dev. Comp. Immunol. 61, 145–153.
Marder, E., Bucher, D., 2007. Understanding circuit dynamics using the stomatogastric nervous system of lobsters and crabs. Annu. Rev. Physiol. 69, 291–316.
Mars Brisbin, M., McElroy, A.E., Pales Espinosa, E., Allam, B., 2015. Antimicrobial activity in the cuticle of the American lobster, *Homarus americanus*. Fish Shellfish Immunol. 44, 542–546.
Maynard, J., van Hooidonk, R., Harvell, C.D., Eakin, C.M., Liu, G., Willis, B.L., Williams, G.J., Groner, M.L., Dobson, A., Heron, S.F., Glenn, R., Reardon, K., Shields, J.D., 2016. Improving marine disease surveillance through sea temperature monitoring, outlooks and projections. Philos. Trans. Biol. Sci. 371 20150208/20150201-20150208/20150211.
Monigatti, F., Gasteiger, E., Bairoch, A., Jung, E., 2002. The Sulfinator: Predicting tyrosine sulfation sites in protein sequences. Bioinformatics 18, 769–770.
Montero-Alejo, V., Acosta-Alba, J., Perdomo-Morales, R., Perera, E., Hernandez-Rodriguez, E.W., Estrada, M.P., Porto-Verdecia, M., 2012. Defensin like peptide from *Panulirus argus* relates structurally with beta defensin from vertebrates. Fish Shellfish Immunol. 33, 872–879.
Montero-Alejo, V., Corzo, G., Porro-Suardiaz, J., Pardo-Ruiz, Z., Perera, E., Rodriguez-Viera, L., Sanchez-Diaz, G., Hernandez-Rodriguez, E.W., Alvarez, C., Peigneur, S., Tytgat, J., Perdomo-Morales, R., 2017. Panusin represents a new family of β-defensin-like peptides in invertebrates. Dev. Comp. Immunol. 67, 310–321.
Petersen, T.N., Brunak, S., von Heijne, G., Nielsen, H., 2011. SignalP 4.0: discriminating

signal peptides from transmembrane regions. Nat. Methods 8, 785–786.
Pisuttharachai, D., Yasuike, M., Aono, H., Yano, Y., Murakami, K., Kondo, H., Aoki, T., Hirono, I., 2009. Characterization of two isoforms of Japanese spiny lobster *Panulirus japonicus* defensin cDNA. Dev. Comp. Immunol. 33, 434–438.
Schindelin, J., Arganda-Carreras, I., Frise, E., Kaynig, V., Longair, M., Pietzsch, T., Preibisch, S., Rueden, C., Saalfeld, S., Schmid, B., Tinevez, J.-Y., White, D.J., Hartenstein, V., Eliceiri, K., Tomancak, P., Cardona, A., 2012. Fiji: an open-source platform for biological-image analysis. Nat. Methods 9, 676–682.
Schmitt, P., Rosa Rafael, D., Destoumieux-Garzon, D., 2016. An intimate link between antimicrobial peptide sequence diversity and binding to essential components of bacterial membranes. Biochim. Biophys. Acta 1858, 958–970.
Shai, Y., 2002. Mode of action of membrane active antimicrobial peptides. Biopolymers 66, 236–248.
Smith, V.J., Dyrynda, E.A., 2015. Antimicrobial proteins: from old proteins, new tricks. Mol. Immunol. 68, 383–398.
Sperstad, S.V., Haug, T., Blencke, H.-M., Styrvold, O.B., Li, C., Stensvaag, K., 2011. Antimicrobial peptides from marine invertebrates: challenges and perspectives in marine antimicrobial peptide discovery. Biotechnol. Adv. 29, 519–530.
Stemmler, E.A., Barton, E.E., Esonu, O.K., Polasky, D.A., Onderko, L.L., Bergeron, A.B., Christie, A.E., Dickinson, P.S., 2013. C-terminal methylation of truncated neuropeptides: an enzyme-assisted extraction artifact involving methanol. Peptides 46, 108–125.
Stepanyan, R., Day, K., Urban, J., Hardin, D.L., Shetty, R.S., Derby, C.D., Ache, B.W., McClintock, T.S., 2006. Gene expression and specificity in the mature zone of the lobster olfactory organ. Physiol. Genomics 25, 224–233.
Tang, Y.Q., Selsted, M.E., 1993. Characterization of the disulfide motif in BNBD-12, an antimicrobial β-defensin peptide from bovine neutrophils. J. Biol. Chem. 268, 6649–6653.
Tsai, P.L., Chen, S.-F., Huang, S.Y., 2013. Mass spectrometry-based strategies for protein disulfide bond identification. Rev. Anal. Chem. 32, 257–268.
Veenstra, J.A., 2000. Mono- and dibasic proteolytic cleavage sites in insect neuroendocrine peptide precursors. Arch. Insect Biochem. Physiol. 43, 49–63.
Yin, H., Killeen, K., 2007. The fundamental aspects and applications of agilent HPLC-chip. J. Sep. Sci. 30, 1427–1434.
Yin, H., Killeen, K., Brennen, R., Sobek, D., Werlich, M., Van de Goor, T., 2005. Microfluidic chip for peptide analysis with an integrated HPLC column, sample enrichment column, and nanoelectrospray tip. Anal. Chem. 77, 527–533.
Zhao, B.-C., Lin, H.-C., Yang, D., Ye, X., Li, Z.-G., 2016. Disulfide bridges in defensins. Curr. Top. Med. Chem. 16, 206–219.